Photophysical Behaviors of Biphenylcarboxylic Acids in Various Solvents; Excited-State Geometry Change and Intramolecular Charge Transfer

Minjoong Yoon*, Dae Won Cho, and Jae Young Lee

Department of Chemistry, Chungnam National University, Taejon 305-764

Minyung Lee and Dongho Kim

Spectroscopy Laboratory, Korea Research Institute of Standards and Science, Taejon 305-606

Received May 1, 1992

The solvent-dependent photophysical properties of 2-biphenylcarboxylic acid (2BPCA) and 4-biphenylcarboxylic acid (4BPCA), which have a pre-twisted conformation in the ground state, have been investigated. The fluorescence spectra of 4BPCA show vibrational structure with a non-mirror image to the absorption spectra in nonpolar solvent while those of 2BPCA show no structure even in nonpolar solvents. As the solvent polarity increases, the fluorescence spectra become diffuse and broad with a strong red shift resulting in the large Stokes shift. The large fluorescence Stokes shift of BPCA's in polar solvent is also partially due to an intramolecular charge transfer (ICT) interaction in the excited state, as demonstrated by the large dipole moment in the excited state (7.6-10.6 D). The fluorescence decay behaviors of BPCA's (decay-times and their pre-exponential factors) also depend on solvent polarity in agreement with the solvent-dependent properties of the steady-state fluorecence. The data have been discussed in terms of change in the excited-state potential energy surface with respect to change of the dihedral angle of biphenyl moiety.

Introduction

There have been great interests for many years in conformational problems of biphenyl and its derivatives[1-6]. In the ground state, the steric repulsion between *ortho* hydrogen atoms of phenyl rings favors a twisted conformation of biphenyl moiety in spite of the π-conjugation of phenyl rings. With electron diffraction methods, the dihedral angle of biphenyl was determined to be 44.4° in the gas phase[1]. Several investigators have also examined the dihedral angle of biphenyl in various solvents. For example, it was determined to be 38° in acetonitrile[2], 40° in benzene[3] and 37° in CS_2[4]. These values show little difference in various solvents even though they are smaller than those in the gas phase, suggesting that the dihedral angle in the ground state is not much influenced by the nature of solvent.

The twisted biphenyl is known to perform geometry change in the first excited singlet state toward a planar conformation by internal rotation around central C-C single bond[6]. The conformational relaxation in much faster than the fluorescence decay time, and the fluorescence originates from the nearly planar conformation only. Because of this conformational change, the fluorescence spectrum of biphenyl shows pronounced structure as compared to the structureless absorption spectrum[6]. Recent CNDO'S calculation and fluorescence spectral studies[7] have showed that the conformational relaxation of biphenyl in the excited state is not hindered in any solvents, as is the ground-state dihedral angle little affected by the nature of solvent. However, a nearly perfect hindrance of the relaxational process was detected for a methyl-substituted biphenyl[7]. This hindrance was suggested to be due to the molecule-solvent interaction in which substituents play an important role. However, it is still far from complete understanding of the solvent effects on the excited-state conformational change of biphenyl derivatives, since a restricted amount of data is accumulated with a limited number of biphenyl derivatives. Furthermore, no systematic experiments have been made to explore the substituent and solvent effects on the excited-state geometry with regard to its relationship to the photophysical properties of biphenyl derivatives. Thus, in this work we have studied the photophysical properties of carboxylic acid-substituted biphenyls such as 4-biphenylcarboxylic acid (4BPCA) and 2-biphenylcarboxylic acid (2BPCA) in various solvents by using the steady-state and time-resolved fluorescence spectroscopy. The carboxylic acid substitution can be expected to affect other photophysical properties by an excited-state change in polarity of the molecule, since the carboxylic group functions as an electron withdrawing group. The observed excited-state behaviors of the biphenyl carboxylic acids (BPCA's) in various solvents have been interpreted in terms of the intramolecular charge transfer (ICT)- state formation and the excited-state geometry change. The formation of ICT state and the geometry change in the excited state has been found to depend on the position of carboxylic acid group and the solvation process.

Experimental Details

Sample Preparation. 2BPCA and 4BPCA were purchased from Aldrich Chemical Co. and purified by repeated recrystallization with ethanol. The melting points of 2BPCA and 4BPCA are in good agreements with the values in reference[8] (114℃ and 226℃, respectively). All the organic solvents used were of spectrograde and further purified and dried as described elsewhere,[9,10]. Buffer solutions were prepared by mixing GR grade acid or base with its salt; KCl-HCl (pH 2), HAc-NaAc (pH 3-5), KH_2PO_4-Na_2HPO_4 (pH 6-8), NH_4

Cl-NH_4OH (pH 9-10). Water was triply distilled in the presence of acidic dichromate and alkaline permanganate. In nonpolar solvents at concentrations much over 0.01 M, carboxylic acids exist as dimers due to hydrogen bonding. Therefore, to avoid the dimerization, the concentrations of the samples prepared in this experiment were kept lower than 2×10^{-5} M.

Spectroscopic Measurements. Absorption spectra were measured on a Beckman UV-5260 spectrophotometer. Steady-state fluorescence measurements were made on a scanning SLM-AMINCO 4800 spectrofluorometer which makes it possible to obtain corrected spectra using Rhodamine B as a quantum counter (excitation slit; 4 nm) as described elsewhere[11]. Fluorescence quantum yields were determined by comparison with a reference of known quantum yield (Indole in methanol, $\Phi_f=0.32$)[12]. The solutions were accurately diluted with the proper solvent to an optical density of not more than 0.05 at the excitation wavelength to eliminate self absorption. A quadratic correction for refractive index variation was applied. All the sample solutions were deaerated before the fluorescence spectral measurements by using freeze-pump-thaw (3-4 cycles down to 10^{-4} torr) method.

The time-resolved fluorescence measurements were made with the picosecond emission apparatus which has been described completely in the recent publication[13]. The fluorescence response functions were produced by using a frequency-doubled-rhodamine-6G dye laser which was pumped by a frequency-doubled mode-locked Nd^{3+} : YAG laser (Coherent Co., U.S.A.) (290 nm; pulse width, 2-3 ps; FWHM, 1 ns; repetition rate, 3.8 MHz), and were detected with a PMT (Hamamatsu R928). The amplified PMT output is collected by a time-correlated single-photon counter developed by using a time-to-amplitude converter (TAC) (EG & G Co. model 457) connected with a constant fraction and leading edge discriminators. The collected signals are digitized by a multichannel analyzer (MCA) (2048 channels). The fluorescence decay parameters were collected on a personal computer by using a MCA data collection program (EG & G Co.), and deconvolution of the instrument response function was performed by using a data analysis software developed at the Laser Center in the University of Pennsylvania. The best fit of the decay was determined by monitoring the value of χ^2 and the distribution of residuals.

Results and Discussion

Solvent Dependence of the Absorption Spectra. Figure 1 shows the absorption spectra of 4BPCA and 2BPCA in different solvents at room temperature. The spectroscopic properties are summarized in Table 1. The absorption spectrum of 4BPCA shows single absorption maximum around 270 nm. The absorption maximum shifts very little as the solvent polarity increases (Figure 1a) and its molar extinction coefficient is very high (10^4 $M^{-1}\cdot cm^{-1}$ order) (see Table 1). These results imply that 270 nm band is attributed to the π, π^* character of biphenyl moiety. The n, π^* character of the carboxyl group is hidden by an extended π-conjugation of biphenyl rings to the neighboring carboxyl group. This is supported by the facts that the absorption maximum of 4BPCA is significantly red-shifted as compared to that of the unsubstitued biphenyl[6] or 4-biphenyl acetic acid (4BPAA)

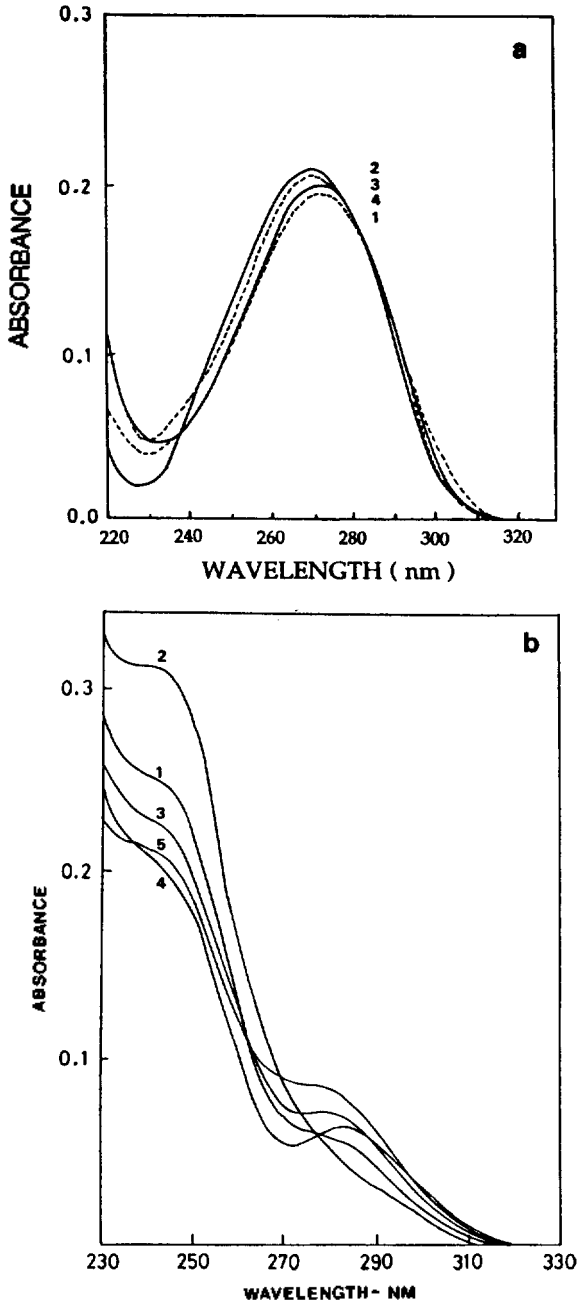

Figure 1. Absorption spectra of 1.0×10^{-5} M 4BPCA (a) and 2.0×10^{-5} M 2BPCA (b) in different solvents: 1=H_2O (pH 3.0); 2=methanol; 3=dioxane; 4=cyclohexane; 5=acetonitrile.

(250 nm) (data not shown).

In contrast to the absorption spectrum of 4BPCA, the absorption spectrum of 2BPCA (Figure 1b) shows two absorption bands around 240 and 280 nm. The 240 nm band has much larger molar extinction coefficient than 280 nm band, indicating that the 240 nm band is attributed to the pure π, π^* transition. However, the 280 nm band is more or less affected by n, π^* transitions. These results may be due to less extended π-conjugation of biphenyl rings to the neighboring carboxyl group in 2BPCA than in 4BPCA probably because of the steric hindrance between the phenyl and carboxyl groups (see below). Little shifts of the absorption maxima (λ_{max}^{ab}) in spectra of both BPCA's in going from nonpo-

Table 1. Absorption Maximum Wavelengths with Molar Absorption Coefficients (ε) of 2BPCA and 4BPCA in Different Solvents

Solvents	2BPCA		4BPCA	
	λ_{max}^{ab}	ε, M^{-1} cm^{-1}	λ_{max}^{ab}	ε, M^{-1} cm^{-1}
Methanol	240	15500	264	25700
	280	1400		
Ethanol	240	12300	265	25100
	280	4000		
Butanol	240	10500	265	24500
	280	4000		
Acetonitrile	240	10700	270	24000
	280	4000		
Dioxane	240	11500	270	33900
	280	3500		
Cyclohexane	240	10000	270	17800
	285	1400		
n-Hexane	240	10000	270	21400
	285	1400		
Water pH 3	240	12600	270	19500
	280	3000		
pH 5	240	15100	264	20400
pH 10	240	15900	264	20400

loar to polar solvents indicate that there are no intramolecular charge transfer interactions (ICT) for both molecules in the ground state.

The pH dependence of the absorption spectra were observed for both BPCA's in the aqueous solution in the pH range, 2-10 (Table 1). The spectrum of 4BPCA at pH 2-3 exhibited the absorption maximum at 270 nm, which resembles that in organic solvents. This indicates that 4BPCA exist in neutral form at pH 2-3. However, the absorption maximum shifts to 264 nm in the pH range higher than 4.0, indicating the formation of anionic species. The same dual absorption maxima of 2BPCA in the acidic solution below pH 4.5 were also oberved as those in organic solvents. However, 280 nm band was not observed above pH 4.5, indicating that both the neutral form and anionic form exist around pH 4.5. The pK_a for the equilibrium between the neutral molecule and anion, determined spectrophotometrically, was found to be 3.46 and 4.25, respecively for 2BPCA and 4BPCA. Because of these pH effects, the aqueous solution used was at pH 3.0 unless otherwise stated, when the solvent effects on the photophysical properties of the neutral carboxylic acids were studied (see below).

Solvent Dependece of the Fluorescence Spectra. Figure 2 shows the fluorescence emission spectra of 4BPCA and 2BPCA in various solvents. In constrast to the weak solvent-dependece of λ_{max}^{ab}, the fluorescence emission maxima (λ_{max}^{em}) are strongly red-shifted as the solvent polarity increases, indicating a possibility of a change in the character of the electronic state, possibly linked to solvent relaxation in the excited state. Furthermore, it is noteworthy that in nonpolar solvent, the fluorescence spectrum of 4BPCA with a maximum at 320 nm has vibrational structure with non-mirror image to the absorption spectrum (see Figure 1a)

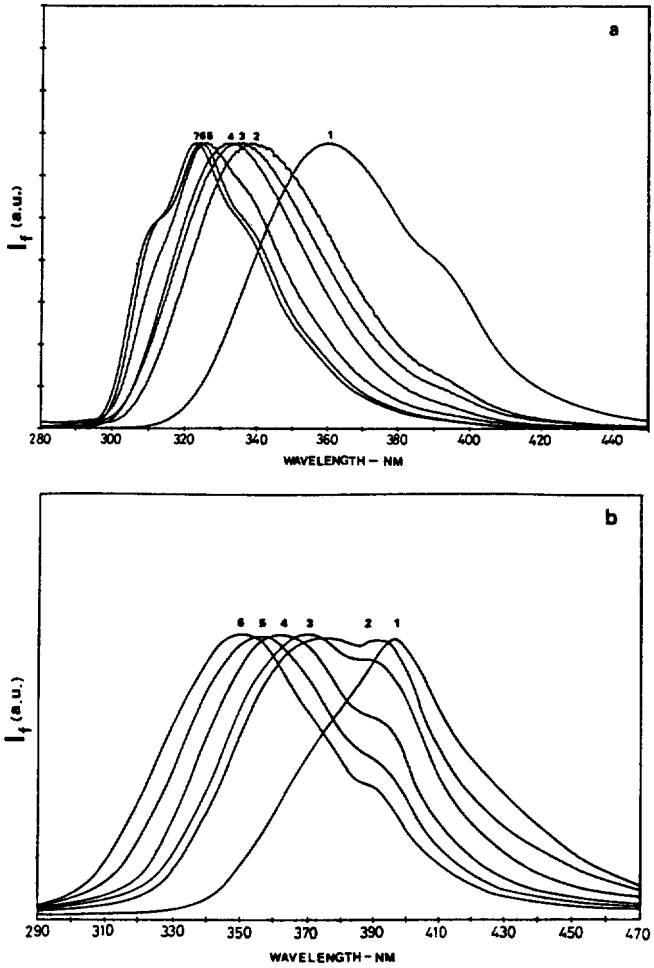

Figure 2. The fluorescence emission spectra of 4BPCA (a) and 2BPCA (b) in different solvents: 1=H_2O (pH 3.0); 2=methanol; 3=ethanol; 4=acetonitrile; 5=dioxane; 6=cyclohexane; 7=*n*-hexane. The emission spectra were measured by excitation at 270 nm and 260 nm, respectively for 4BPCA and 2BPCA. They are normalized arbitrally.

as in the case of unsubstituted biphenyl[6], implying that the molecular geometry change takes place in the excited state toward coplanar conformation by internal rotation around the central C-C bond. With increasing polarity of solvent, the fluorescence spectrum shows loss of the vibrational structure, exhibiting the diffuse and broad shape with the large red shift of the emission maximum. This suggests that the excited-state geometry change toward coplanar conformation is hindered in polar solvent through a molecule-solvent interaction with the subsequent solvent relaxation. In other words, the biphenyl moiety of the excited 4BPCA in polar solvent would remain as twisted as in the ground state. Such solvent effects on the fluorescence spectrum were not observed for the unsubstituted biphenyl[6] and the 4BPAA (data not shown). These results indicate that the extended *π*-conjugation of biphenyl to the carboxyl group seems to play an important role in the interaction with polar solvent to hinder the internal rotation of the biphenyl moiety in the excited state of 4BPCA. The extended *π*-conjugation would induce an excited-state resonance contribution of the substituent carboxyl group to the benzene ring shown as **I**, resulting in the in-

creased polarity to facilitate the interaction with polar solvents. Hence protonation of the carbonyl oxygen in coplanar with the benzene ring should be also facilitated in the excited state. Thus, the carboxylic acid substitution may result in stronger solvation of 4BPCA in the excited state *via* intermolecular excited-state hydrogen-bonding (see below), as demonstrated by the very large Stokes shift in protic polar solvent than in aprotic polar solvent.

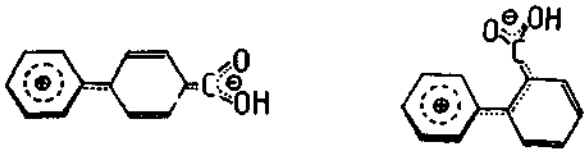

I II

Figure 2(b) shows the fluorescence emission spectra of 2BPCA in different solvents at room temperature. In contrast to the fluorescence spectrum of 4BPCA, the vibrational structure was not clearly observed even in non-polar solvent as well as in polar solvent, indicating lack of the molecular geometry change toward coplanarity of the biphenyl moiety in the excited state. This may be due to greater steric hindrance between phenyl ring and the *ortho* carboxyl group as compared to the steric hindrance of hydrogen atoms of the unsubstituted biphenyl. Actually, the results of theoretical calculation (MM2 method) show that the ground-state dihedral angle of the biphenyl moiety of 2BPCA (53.80°) is significantly larger than that of 4BPCA (39.44°) (to be published separately). In protic polar solvents, the fluorescence Stokes shift is extraordinarilly larger (8000-105000 cm^{-1}) than in aprotic polar solvent as in the case of 4BPCA. These results also indicate the presence of the strengthened hydrogen bonding between the carboxyl group and the protic solvent due to the excited-state resonance contribution of the carboxyl group (see the structure II above).

The large Stokes shift of the λ_{max}^{em} of BPCA's in polar solvent may be also due to the increase of dipole moments or polarities in the excited state. This implies the formation of the intramolecular charge transfer (ICT) state (benzene as an electron donor and benzoic acid as an acceptor) in the excited state, being consistent with the excited-state resonance contribution as dicussed above. If the molecule-solvent interaction is primarily of a dipole-dipole characteristics, the Stokes shift ($\nu_a - \nu_f$) is dependent on the solvent polarity parameters, $[(\varepsilon-1)/(2\varepsilon+1)-(n^2-1)/(2n^2+1)]$ as expressed in the following Eq. (1)[14],

$$\nu_a - \nu_f = \frac{2}{hc} \times \left(\frac{\varepsilon-1}{2\varepsilon+1} - \frac{n^2-1}{2n^2+1}\right) \times \frac{(\mu_e-\mu_g)^2}{a^3} + \text{constant} \quad (1)$$

where μ_g and μ_e are the dipole moments of the molecule in the ground state and in the lowest excited single state, respectively, h is Planck constant, c is the speed of light in vaccum and "a" is the Onsager radius cavity. Figure 3 shows the plot of Eq. (1) *i.e.*, Stokes shifts of 2BPCA and 4BPCA as a function of the polarity parameters of several solvents. The line is drawn through the circled points which represent data for the molecules in aprotic solvents. From the slope, the value of $\mu_e - \mu_g$ can be evaluated with a known value of "a" parameter. From key bond length and bond angles evaluated by X-ray analysis on 4-hydroxybiphenyl[15]

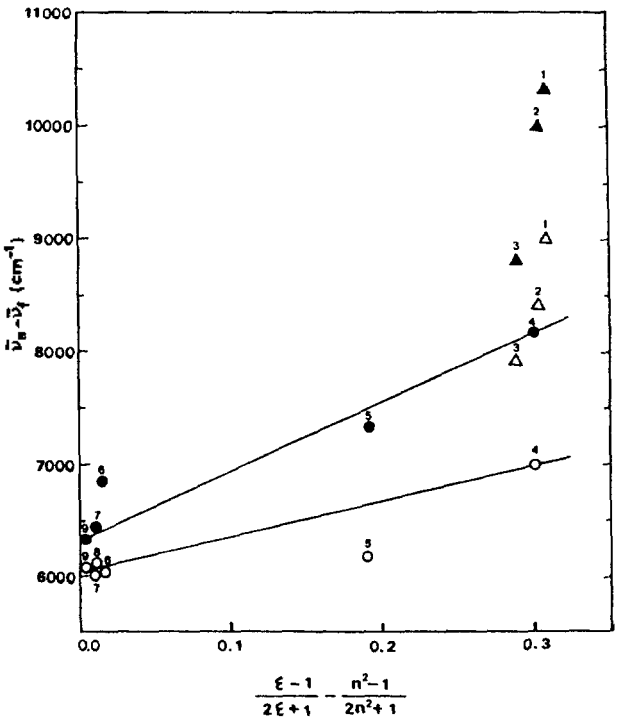

Figure 3. The Stokes shift of 4BPCA (open circle and triangles) and 2BPCA (dark circle and triangles) fluorescence as a function of solvent polarity parameters. The numbers refer to the following solvents; 1=H_2O (pH 3.0); 2=methanol; 3=ethanol; 4=acetonitrile; 5=N,N-dimethylformamide; 6=chloroform; 7=ethyl ether; 8=dioxane; 9=cyclohexane; 10=benzene; 11=*n*-hexane.

and Fisher-Hershfield-Taylor models, the "a" value is approximated to be 5 Å. The evaluated values of $\mu_e - \mu_g$ are 9.0 D and 6.0 D, respectively for 2BPCA and 4BPCA. Assuming μ_g is 1.64 D as that of benzoic acid[16], the μ_e's for 2BPCA and 4BPCA are determined to be 10.6 D and 7.6 D, respectively. The μ_e value for 2BPCA is close to the expected dipole moment for full electron transfer (13.9 D) which is calculated by treating the donor and acceptor as point charges with the distance taken from the center of benzene to the center of benzoic acid. This supports the possibility of the excited ICT interaction in 2BPCA. However, the μ_e for 4BPCA is a little far from the expected value, indicating that the formation of the excited ICT state is not as feasible in 4BPCA as in 2BPCA.

In spite of the possibility of the ICT interaction in the excited state, 2BPCA does not exhibit any markedly dual emissions from the initially excited state and the ICT state even in highly polar (aprotic) solvent such as acetonitrile. However, it is noteworthy that the fluorescence spectrum of 2BPCA in methanol exhibits the increased intensity of the emission band around 400 nm in addition to the 360 nm (see Figure 2b). Furthermore, in the aqueous solution at low pH (1-3) where 2BPCA exist in neutral form, the 400 nm emission is dominant. In going from methanol to propanol, the 400 nm emission decreases with an increase of the 360 nm. These observations suggest that the 400 nm emission is partially attributed to the ICT state relaxed from the initially excited state, indicating that the ICT process of 2BPCA is influenced by the strengthened intermolecular

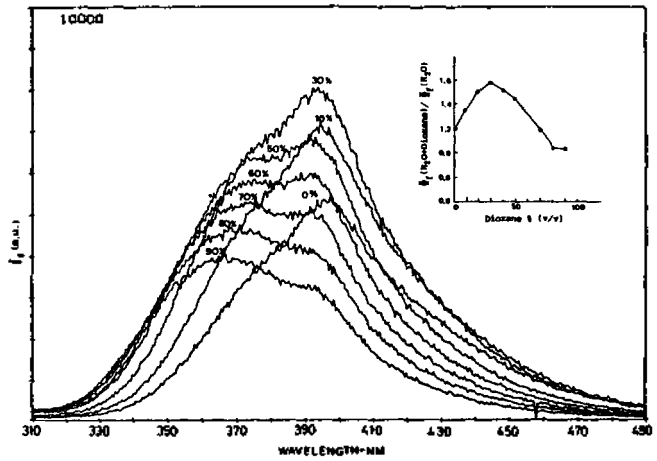

Figure 4. Fluorescence emission spectra of 2BPCA in water-dioxane mixture solvents with relative proportions of dioxane. The inset exhibits the relative quantum yield of the fluorescence of 2BPCA as a function of the solvent composition.

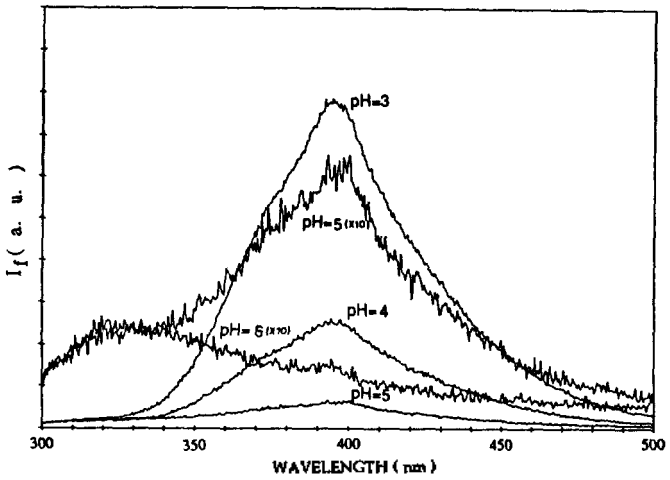

Figure 5. Fluorescence spectra of 2BPCA in aqueous solutions of different pH.

hydrogen-bonding in the excited state. Supporting this, the fluorescence spectrum in the aqueous solution is changed sensitively upon addition of dioxane (Figure 4), showing dual emission in the dioxane-water mixture and two types of responses of the fluorescence quantum yield to increasing solvent polarity (Inset in Figure 4). These results are similar to those of other ICT molecules such as 2-N-arylamino-6-naphthalene sulfonates[17].

In order to confirm the strengthened intermolecular hydrogen-bonding in the excited state, the fluorescence spectral changes were observed in the pH range, 3-10 (Figure 5). From these results and the absorption spectral data, the excited state pK_a^* were determined by using Foerster cycle method[18]. The pK_a^* of 2BPCA is 13.00, which is much larger than the pK_a (3.46), being consistent with the argument that the basicity of the aromatic acids are more strengthened in the excited state[19]. The pK_a^* of 4BPCA (9.80) was also determined to be larger than pK_a (4.25), even though its difference from pK_a is not as large as the corresponding difference for 2BPCA. A migration of electron density from

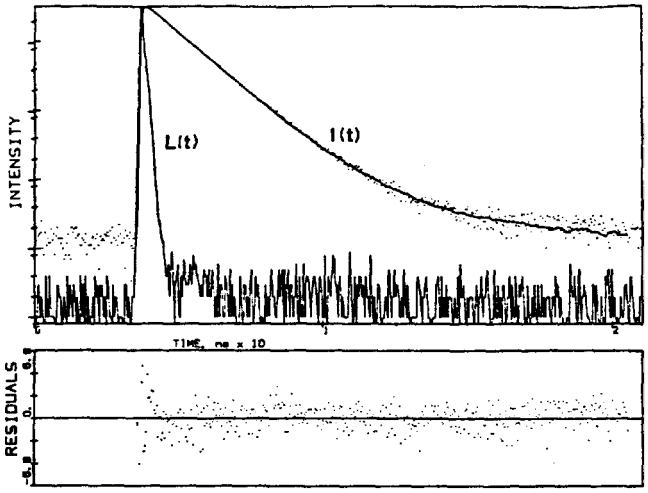

Figure 6. Fluorescence responce function I(t)'s of 4BPCA in cyclohexane produced by a mode-locked Nd^{3+} : YAG laser-pumped pulsed dye laser (290 nm). They were monitored at 326 nm and obtained by the single photon counting method at the ambient temperature. L(t) is the instrument response function (FWHM, 1 ns).

the benzene ring to the carboxyl group would produce the excited-state resonace contribution to the facilitated protonation of the carboxyl group as in the case of 9-methyl anthroate[20]. The strongest hydrogen bonding would be formed between water and carboxyl group so that the carboxyl group becomes coplanar with benzene ring. Thus, the steric hindrance between the benzoic acid and the phenyl group of 2 BPCA would be rather enhanced by the excited-state hydrogen-bonding interaction, keeping the biphenyl moiety further twisted in the excited state so that the back electron transfer is inhibited after the excited-state ICT interaction. This consideration is quite similar to the recent findings[21] that the excited-state intramolecular electron transfer in 4-(dialkylamino) pyrimidines is favored by the hydrogen bonding to the pyrimidine nitrogen. The hydrogen bonding is known to increase the steric hindrance between the alkylamino group and the pyrimidine moiety, reducing the energy barrier for formation of the twisted ICT state. However, the phenyl group of 4BPCA is in *para*-position to the carboxyl group, and one cannot expect the enhanced steric hindrance as in 2BPCA. Therefore, the dihedral angle of the biphenyl moiety of the excited 4BPCA remains relatively unchanged as compared with that of 2BPCA, even though the rotational relaxation toward coplanarity of the biphenyl moiety is at least inhibited by the molecule-solvent interaction in polar solvents. The small dihedral angle (*ca.* 39°) of 4BPCA may not be large engough to prevent the back electron transfer. This is the reason why 4BPCA does not shown the ICT emission band clearly even in the aqueous solution.

In order to further understand the excited-state geometry change and the ICT process of 2BPCA, we have measured the fluorescence quantum yields and the picosecond time-resolved fluorescence decays of BPCA's in different solvents. The fluorescence quantum yields of BPCA's measured are listed in Table 2. The fluorescence quantum yields of 4BPCA are higher in nonpolar solvents than in polar solvents. This

Table 2. Fluorescence Quantum Yields (Φ_f) and Decay Times (τ) of 2BPCA and 4BPCA in Various Solvents

Solvents	2BPCA				4BPCA			
	Em[a] (nm)	Decay times,[b] ps		Φ_f[c]	*Em*[a] (nm)	Decay times,[b] ps		Φ_f
Methanol	350	580 (66)	3360 (34)	0.01	340	880		0.11
	400	570 (83)	2900 (16)					
Ethanol	350	500 (90)	3280 (10)	0.01	340	500		0.13
Acetonitrile	350	340		0.02	340	210		0.14
Dioxane	350	270		0.02	330	110		0.15
Cyclohexane	350	250		0.03	326	80 (35)	1260 (65)	0.31
Water pH 3	350	700 (56)	1610 (44)	0.01	360	1700		0.14
	400	680 (62)	1630 (38)					

[a] *Em* represents the monitoring emission wavelength. [b] Estimated errors = ± 5%; The value in paranthesis represent the amplitude (%) of each component of the biexponential decay. [c] Estimated errors = ± 10%.

may be due to the increased π, π^* character in the S_1 state by the excited-state geometry change toward the coplanarity of the biphenyl moiety. The fluorescence quantum yields of 2BPCA are significantly smaller than those of 4BPCA, supporting the less extended π-conjugation of the biphenyl moiety of the *ortho*-carboxyl group as compared to 4BPCA because of the steric hindrance. Figure 6 shows the typical fluorescence decay functions I(t) of 4BPCA in cyclohexane monitored at 326 nm, together with the instrument response function L(t). The fluorescence decay times obtained by analyzing I(t)'s of 4BPCA in various solvents are summarized in Table 2. The fluorescene decay of 4BPCA in cyclohexane is clearly resolved into two exponential components. Considering the possibility of the excited-state geometry change as discussed above, the fast decay component (80 ps) and the slow decay component (1260 ps) may originate from the twisted conformation and the relaxed coplanar conformation, respectively. The amplitute of the fast component of 4BPCA in cyclohexane (35%) is smaller than that of the slow component (65%), being in good agreement with the inference that the twisted conformation of 4BPCA in the ground state is mostly changed into the coplanar conformation upon excitation. Thus, the decay time of the fast component may be comparable to the relaxation time of the internal rotation around the central C-C bond of biphenyl moiety for the excited-state geometry change toward coplanarity. The fluorescence decay becomes single exponential and the decay time increase significantly as the polarity and hydrogen bonding ability of the solvent increase (see Table 2) in parellel with the red-shift of the fluorescence spectrum, indicating that the relaxational process for the geometry change in the S_1 state is inhibited due to the molecule-solvent interaction.

The fluorescence decay of the cyclohexane solution of 2 BPCA is single exponential with the decay time (260 ps) in contrast to the biexponential decay of the corresponding 4BPCA solution (Table 2). This indicates that the relaxational process for the excited-state geometry is inhibited even in nonpolar solvent in agreement with the interpretation of the fluorescence spectrum, supporting the conclusion that the twisted geometry of biphenyl moety of 2BPCA is relatively well maintained in the excited state because of the steric hindrance. The decay time increase gradually as the solvent polarity increases too, and it seems to keep the molecule-solvent interaction effective for the inhibition of the excited-state geometry change as in 4BPCA. Then it is interesting to note that the fluorescence decay of 2BPCA becomes biexponential with the slower decay time in protic polar solvents in contrast to the single exponential decay of 4BPCA. This indicates the presence of two excited states such as the initially excited state and the relaxed state. Since the slower decay component is obtained in the hydrogen-bonding, the relaxed state which is responsible for the slow decay component would be attributed to the further-twisted conformation formed through the intermolecular hydrogen bonding in the excited state as discussed above. The slow decay time is even smaller (1610 ps) in water than in methanol. If we assume that the fluorescence quantum yields of the initially excited species and the relaxed species are proportional to the overall quantum yields by the amplitude of each decay component in both methanol and aqueous solutions, the radiative decay constant (k_r) and nonradiative decay constant (k_{nr}) can be calculated by using the following equations,

$$k_r = \phi_f/\tau_f \tag{2}$$

$$k_{nr} = (1-\phi_f)/\tau_f \tag{3}$$

where ϕ_f and τ_f are the fluorescence quantum yield and decay time, respectively. According to this calculation, the nonradiative decay constant in the aqueous solution is larger than that in methanol; $k_{nr} = 6.14\times10^8$ sec^{-1} in water, 2.80×10^8 sec^{-1} in methanol. However, the radiative decay constants show little difference; $k_r = 1.0\times10^7$ sec^{-1} in water, 1.2×10^7 sec^{-1} in methanol. Such solvent dependence of the k_r and k_{nr} have been commonly observed for other ICT molecule such as (phenylamino) naphthalenesulfonates[17]. Thus, these results should be due to the partial contribution of the ICT interaction.

Possible Potential Surface. The above observations suggest that the excited-state potential surface connecting the twisted conformation and the coplanar conformation of BPCA's is dependent on the solvent polarity (or hydrogen-bonding ability) and position of the substituent as shown in Figure 7. As for 4BPCA, in nonpolar solvent the ground-state twisted conformation having 39.44° dihedral angles is changed into the coplanar conformation rapidly upon excita-

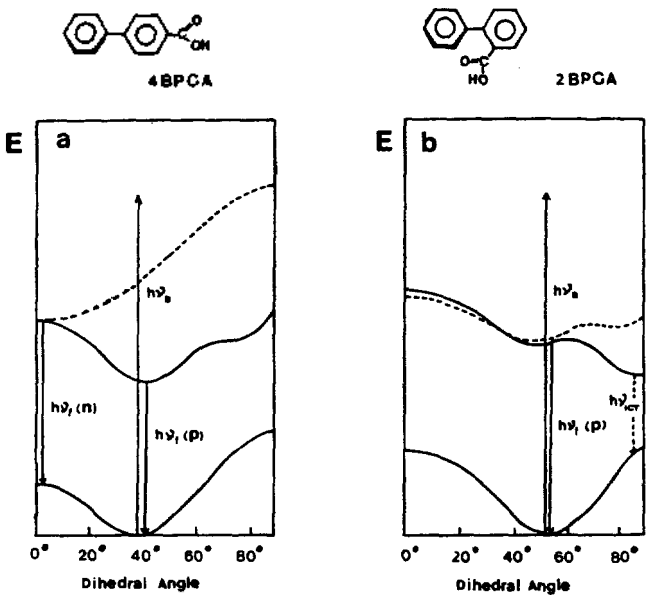

Figure 7. Schematic representation of ground- and excited-state potential surfaces for 4BPCA (a) or 2BPCA (b) undergoing solvent-dependent geometry changes and ICT-state formation. $h\nu_f$ (p), $h\nu_f$ (n) and $h\nu_{ICT}$ represent emissions from the locally excited state, the coplanar conformation and ICT state, respectively. The dotted and solid lines represent the excited-state potential surfaces in the nonpolar and protic polar solvents, respectively.

tion as in the case of the unsubstituted biphenyl (see dotted line in Figure 7a). However, in polar solvent the excited 4BPCA shows a partial hindrance of the internal rotation around the central C-C bond of the biphenyl moiety by the molecule-solvent interaction. Thus, the ground-state twisted conformation remains even in the excited state, but the barrier hieght for further twist relaxation is relatively high so that the formation of stable ICT state is inhibited. Thus, only normal emission is available from the initially excited state of 4BPCA.

However, the excited 2BPCA shows a partial hindrance of the internal rotation even in nonpolar solvent because of the steric hindrance. Especially in protic polar solvent, the rotational hindrance would be enhanced, and the further twist of the biphenyl moiety may be possible through the enhanced hydrogen-bonding of the *ortho* carboxyl group with protic solvent. Therefore, the relaxation process for the formation of ICT state of 2BPCA is more feasible than 4BPCA. Nonetheless, the magnitude of the dipole moment of the ICT state of 2BPCA is about 76% of the expected values for full charge separation to occur at the 90° twist angle. Accordingly, the ICT fluorescence of 2BPCA would be occurring from geometry with dihedral angle less than 90°. This is probably the reason why the valley around 380 nm on the dual emission of 2BPCA in methanol is not so deep (Figure 2b) as in the case of typical twisted ICT molecules which are known to be orthogonaly twisted before emitting[22-25].

Conclusion

This work demonstrates that the anomalous fluorescence properties of 2BPCA in polar solvents are due to the partial contribution from the ICT interaction in competition with the geometry change of the biphenyl moiety toward coplanarity in the excited state. The pretwisted structure of the biphenyl moiety of 2BPCA in polar protic solvent seems to be further twisted upon excitation because of the enhanced steric hindrance with *o*-carboxyl group through the hydrogen-bonding interaction with solvent. Therefore, the ICT emission can be more clearly observed in the aqueous solution than in other solvents. These results are similar to the earlier speculations[20,26] that the excited-ICT process is controlled by the local short range solute-solvent interaction as well as the long range polarization interaction. However, the steric hindrance for 4BPCA in the excited state is not affected by the hydrogen-bonding interaction so that the dihedral angle of the biphenyl moiety remains relatively unchanged as compared with that of 2BPCA.

Acknowlegement. This work has been supported by the Basic Science Research Institute Program, Ministry of Education of Korea (BSRI-90-319) and the Korea Science and Engineering Foundation (91-03-00-03).

References

1. A. Almenningen, O. Bastiansen, L. Fernholt, B. N. Cyvin, S. J. Cyvin, and J. J. Samdal, *J. Mol. Struct* **128**, 59 (1985).
2. K. Z. Mobius, *Natureforsch. A: Astrophys. Phys. Phys. Chem.*, **20**, 1117 (1965).
3. I. A. Bogdanov and M. F. Vuks, *Zh. Fiz. Khim.*, **3**, 46 (1965).
4. A. Minoru, T. Watanabe, and M. Kakihana, *J. Phys. Chem.*, **90**, 1752 (1986).
5. T. Seiji and K. Tanabe, *J. Phys. Chem.*, **95**, 139 (1991).
6. I. B. Berlman and O. J. Steingraber, *J. Phys. Chem.*, **75**, 318 (1971).
7. G. Swiatkowski, R. Menzel, and W. Rapp, *J. Luminescence*, **37**, 183 (1987).
8. Dictonary of Organic Compounds, 5th ed., Vol. 1, 1982, Chanpman and Hall, New York.
9. D. McMarrow and M. Kasha, *J. Phys. Chem.*, **88**, 2235 (1984).
10. G. A. Brucker and D. F. Kelley, *J. Phys. Chem.*, **91**, 2863 (1987).
11. J. R. Lakowicz, "Principles of Fluorescence Spectroscopy", Chapter 2, Plenum Press, New York, 1983.
12. E. P. Kirby and R. F. Steiner, *J. Phys. Chem.*, **74**, 4480 (1970).
13. D. Kim and M. Lee, *J. Opt. Soc. Korea*, **1**, 52 (1990).
14. N. Mataga, Y. Kaifu, and M. Koizumi, *Bull. Chem. Soc. Jpn.*, **29**, 465 (1956).
15. C. P. Brock and G. L. Morelan, *J. Phys. Chem.*, **90**, 5631 (1986).
16. A. J. Gordon and R. A. Ford, The Chemist's Companion, John Wiley & Sons, New York, 1972.
17. E. M. Kosower, *Accounts Chem. Res.*, **15**, 259 (1982).
18. Th. Foerster, *Z. Electrochem.*, **54**, 531 (1950).
19. R. S. Becker, "Theory and Interpretation of Fluorescence and Phosphorescence", Wiley Interscience, New York, pp. 239, 1969.
20. T. C. Werner and R. M. Hoffman, *J. Phys. Chem.*, **77**, 1611 (1973).

21. J. Herbich, Z. R. Grabowski, H. Wojtowicz, and K. Golankiewicz, *J. Phys. Chem.*, 93, 3439 (1989).
22. W. Rettig and G. Wermuth, *J. Photochem.*, 28, 351 (1985).
23. Z. R. Grabowski, K. Rotkiewicz, A. Siemiaczuk, D. J. Cowley, and W. Bauman, *Nouv. J. Chim.*, 3, 443 (1979).
24. W. Rettig and W. Zander, *Ber. Bunsen-Ges. Phys. Chem.*, 87, 1143 (1983).
25. D. W. Anthon and J. H. Clark, *J. Phys. Chem.*, 91, 3530 (1987).
26. Y. Wang and K. B. Eisenthal, *J. Chem. Phys.*, 77, 6076 (1982).

Study of the Optimization and the Depth Profile Using a Flat Type Ion Source in Glow Discharge Mass Spectrometry

Jin Chun Woo*, Hyo Jin Kim†, Heoung Bin Lim, Dae Won Moon, and Kwang Woo Lee

Inorganic Analytical Chemistry Lab., Korea Research Institute of Standards and Science, Taejon 305-606
†Department of Pharmacy, Dong Duck Women's University, Seoul 136-714
Received May 12, 1992

The analytical performance of glow discharge mass spectrometer (GD-MS), using a flat type ion source is discussed. The efficiency of ion extraction was maximized at the distance between anode and cathode of 6 mm. At the operation condition of 4 mA, −1000 volt, and 1 mbar for the source, the optimum voltages for sampler and skimmer were 40 volt and −280 volt, respectively. The intensities of Cu, Zn, and Mn were increased as a function of square root of current approximately. Korea standard reference materials (KSRM) were tested for an application study. The detection limits of most elements were obtained in the range of several ppm at the optimized operating condition. The peaks of aluminum and chromium were interfered by those of residual gases. The depth profile of nickel coated copper specimens (3, 5, 10 μm thickness) were obtained by plotting time versus intensities of Ni and Cr after checking the thickness of nickel coated using a scanning electron microscope (SEM). At this moment, the sputtering rate of 0.2 μm/min at the optimum operating condition was determined from the slope of the plot of time to the coating thickness. The roughness spectra of specimen's crater after 16 min. discharge were obtained using a Talysuf5m-120 roughness tester as well.

Introduction

As one of the inorganic analytical techniques, the glow discharge mass spectrometry (GD-MS) has been studied for a long time. The glow discharge technique is simple because a bulky solid sample can be directly analyzed without any sample preparation and free from the concommitant interference due to its unique plasma generation mechanism, *i.e.*, sputtering, not thermal process. Even though, the glow discharge technique has the recognition as a relatively very old, compared with other plasma sources, it has many attentions from analytical scientists for an ultimate atomic spectrometer. Its application field is expanding quickly owing to the developmemt of Radio Frequency Glow Discharge Source Mass Spectrometry (RF-GDMS) which makes it possible to analyze the nonconducting samples. Marcus *et al.*[12] use the 13.56 MHz RF generator to supply the discharge operating potential and the electrically insulating material such as glasses and ceramics were analyzed. The operating pressure of RF-GD is 100-500 mTorr which is relatively lower than that of conventional DC-GD of 1-10 Torr.

Also, Glow Discharge Source has been increasingly applied for studying the chemical composition of solid surfaces and thin film systems. This is due to the minimal sample preparation requirements, good depth resolution, and wide dynamic range. However, most of researches for the in-depth analysis with the glow discharge have been studied by the optical method. Belle *et al.*[3] analysed the metal alloys in depths of 0.1 to 40 μm with a glow discharge source for optical emission spectrography. Greene *et al.*[4-7] determined boron impurity profiles in silicon, measuring the concentration and distribution of constituents in semiconductor films, and the depth information in solid samples. Waitlevertch *et al.*[8] operated a glow discharge with a constant dc mode or a square wave dc mode, but better repriducibility and accuracy have been achived with the square-wave dc mode. Pons-Corbeau et al.[9,10] studied the quantitative determination of variations of composition in galvanized coatings and for an estimation of the enrichments on the surface of annealed extra mild steel sheets with GD-OES. They also show that the emission yield of an element is independent of the matrix although particular phenomena can affect the apparent experimental values. Bengton[11] investigated the variation in intensity of Ar I lines in order to exclude the influence of the sample sputtering rate, and compared with the sample sputtering rate. He concluded that the number density of the sample atom in the plasma saturates with increasing voltage. Nickel *et al.*[12] applied the various glow discharge mode to find optimum conditions for the transformation of intensity-time profiles into concentration-depth dependencies using the alloy matrix as a reference. Element concentrations were calcul-